

Contract No:

This document was prepared in conjunction with work accomplished under Contract No. DE-AC09-08SR22470 with the U.S. Department of Energy.

Disclaimer:

This work was prepared under an agreement with and funded by the U.S. Government. Neither the U. S. Government or its employees, nor any of its contractors, subcontractors or their employees, makes any express or implied: 1. warranty or assumes any legal liability for the accuracy, completeness, or for the use or results of such use of any information, product, or process disclosed; or 2. representation that such use or results of such use would not infringe privately owned rights; or 3. endorsement or recommendation of any specifically identified commercial product, process, or service. Any views and opinions of authors expressed in this work do not necessarily state or reflect those of the United States Government, or its contractors, or subcontractors.

STRUCTURAL ANALYSES OF FUEL CASKS SUBJECTED TO BOLT PRELOAD, INTERNAL PRESSURE AND SEQUENTIAL DYNAMIC IMPACTS

Tsu-te Wu
Savannah River National Laboratory
Aiken, South Carolina 29803

ABSTRACT

Large fuel casks subjected to the combined loads of closure bolt tightening, internal pressure and sequential dynamic impacts present challenges when evaluating their performance in the Hypothetical Accident Conditions (HAC) specified in the Code of Federal Regulations Title 10 Part 71 (10CFR71). Testing is often limited by cost, difficulty in preparing test units and the limited availability of facilities which can carry out such tests. In the past, many casks were evaluated without testing by using simplified analytical methods. In addition, there are no realistic analyses of closure bolt stresses for HAC conditions reported in the open literature.

This paper presents a numerical technique for analyzing the accumulated damages of a large fuel cask caused by the sequential loads of the closure bolt tightening and the internal pressure as well as the drop and crash dynamic loads. The bolt preload and the internal pressure are treated as quasi-static loads so that the finite element method with explicit numerical integration scheme based on the theory of wave propagation can be applied. The dynamic impacts with short durations such as the 30-foot drop and the 40-inch puncture for the hypothetical accident conditions specified in 10CFR71 are also analyzed by using the finite-element method with explicit numerical integration scheme.

INTRODUCTION

This paper presents a new methodology for analyzing the cumulative damage in fuel casks subjected to the closure bolt tightening preload, internal pressure, 30-foot drop and 40-inch puncture which are sequentially applied. The methodology utilizes the import technique of the finite-element mesh and the analytical results from one dynamic analysis using explicit numerical integration scheme into another dynamic analysis also using explicit numerical integration scheme. This methodology has the following advantages over the conventional method:

1. The stresses due to the bolt-tightening preload can be effectively incorporated into the analyses for the subsequent loading;
2. The bolt stresses caused by each sequential event, such as bolt-tightening preload, internal pressure and impact loads can be more accurately calculated;
3. The initial velocity of each sequential event in the Hypothetical Accident Conditions (HAC) can be directly defined.
4. The finite-element model of a system component such as an unyielding floor or a punch bar can be added for an impact simulation or removed to avoid obstruction in the impacting path.

To illustrate the analytical procedures involved in this methodology, the example problem of a shipping cask subjected to the sequential loading of a 30-foot drop followed by a 40-inch puncture was simulated. The effect of the bolt-tightening preload and internal pressure was also accounted for. Since the example

problem is used only for illustration purpose, it does not represent an actual cask design either in structural components or geometrical configuration.

ANALYSIS

The example problem to illustrate the new methodology consists of three separate but sequential finite-element analyses using explicit numerical integration scheme; namely, the first analysis for closure bolt tightening, the second analysis for the 30-foot drop and the third analysis for the 40-inch puncture. The advantages of performing three separate analyses instead of a single analysis together with utilizing the import technique are given in the preceding section. The methodology is discussed in details in the following subsections.

First Analysis for Bolt Preload and Internal Pressure

The new methodology models the closure-tightening process as a quasi-static (slow dynamic) process. By treating the closure-tightening process as dynamic instead of static, the explicit integration method based on the wave propagation theory is applicable. As a result, the complex conditions of contact interfaces among the package components can be effectively simulated. In addition, since the dynamic simulations for the hypothetical accident conditions of shipping casks are mostly performed using the explicit integration method, the proposed methodology for the closure-tightening simulation can be easily incorporated into the simulations for the subsequent drop and puncture loadings. A connector finite-element model is used to monitor the bolt force and the relative displacement between the bolt threads and the flange threads. The bolt force in the connector element model is initially treated as an applied negative force to pull the bolt threads toward the flange threads. After the bolt force reaches the magnitude of the desired bolt preload, the connector element displacement is locked and the bolt load is removed. As a result, the applied bolt load is converted from a surface force to a self-limiting body force.

The analytical results of this sample problem indicate that this methodology generates more accurate stress and strain distribution and magnitudes in closure-joint regions than conventional methods.

The present methodology includes the following multiple advantages over the existing methods:

1. The bolt preload is treated as a residual body force which is representative of the physical system. Thus, the stress distribution and magnitudes of the residual body force can be more accurately determined.
2. It can account for the combined effect of the bolt preload, the internal and external applied loads, the prying load and bending moments as well as the thermal loads.
3. It can be easily incorporated into the subsequent dynamic simulations for the sequential loads in the hypothetical accident conditions.

Finite-Element Model

Figure 1 shows the analyzed finite-element model. Since the geometrical configuration and the loading conditions are symmetric with respect to a certain plane passing through the axis of the package, the finite-element model need only include one half of the package.

The finite-element models of the package components are all comprised of three dimensional (3D) solid elements (Type C3D8R in the ABAQUS finite-element computer program [2]).

Although the applied loads including the bolt-tightening preloads and internal pressure in the present analysis are all axially symmetrically distributed, one half of the package is modeled so that the analytical results can be incorporated into the possible subsequent analyses for the hypothetical conditions.

The uni-axial connector model (Figure 2) is used to simulate the bolt-tightening process. The nodes in the regions of the engaged threads in the bolt and in the flange bolt hole are respectively constrained to two

separate reference points. The tightening force and the relative displacement between the engaged threads in the bolt and the engaged threads in the flange can then be simulated by the connector element between the two reference points.

Applied Loads

The maximum values of the bolt-tightening load at each model of the full bolt is 3000 lbs and at each model of the one-half bolt is 1500 lbs; namely;

$$CCF1_{, \max} = 3000 \text{ lbs} \quad \text{for full bolt models (1)}$$

$$CCF1_{, \max} = 1500 \text{ lbs} \quad \text{for half bolt models (2)}$$

The maximum value of the internal pressure is:

$$P = 500 \text{ psi} \quad (3)$$

Boundary and Contact Conditions

Symmetric boundary conditions are applied to the symmetric plane. The bottom end of the cask is also fixed. The contact conditions between the interfaces of the components are simulated by using the general contact options and the penalty method available in ABAQUS Code.

Analytical Procedures

To determine the structural responses of the package subjected to the sequential loading of the bolt preload and the internal pressure, the analysis consists of the following two load steps.

The first load step is to analyze the structural response of the package during the bolt-tightening process. A negative connector force, $-CCF1$, is applied between the reference points in accordance with the smooth function shown in Figure 3. As long as the connector force (the bolt-tightening force) reaches the desired value of -3000 lbs for the full bolt model and -1500 lbs for the half bolt model, the connector is locked. There will be no more relative displacements between the two reference points after the connector is locked. As a result, this locking condition represents the engagement of the threads in bolt and those in the bolt hole.

During the second load step, the internal pressure of 500 psi is gradually applied on the inner surfaces of the containment vessel in accordance with the function shown in Figure 4.

Second Analysis for 30-Foot Drop

The second analysis is to evaluate the structural responses of the cask to a 30-foot lateral drop. The finite-element model of the unyielding floor is added in this analysis as shown in Figure 6.

Boundary and Contact Conditions

The boundary conditions can not be imported from the previous results and must be redefined in the present analysis. The symmetric boundary conditions are applied to the symmetric plane. Since the floor is unyielding, all the nodes are assumed to be fixed.

The uni-axial connectors which simulate the bolt-tightening forces and thread engagement motions in the first analysis are locked in position after the preloads are fully applied. Thus, the displacements of the uni-axial connectors should remain constant during the present analysis; namely,

$$CU1 = 0 \quad (3)$$

The contact conditions between the interfaces of components are simulated by using the general contact conditions and the penalty method available in the ABAQUS computer code [2].

Initial Velocity and Applied Loads:

The present analysis for the 30-foot drop is not a continuation of the previous analysis discussed above. Rather, the analytical results imported from the previous analysis are treated as the initial state of the present analysis. As a result, the initial velocity of the cask corresponding to the 30-foot free drop can be directly defined in this analysis.

The cask model is initially located near the target floor so that the initial velocity is equal to the velocity of the cask after a 30-foot free fall. The falling path is along the global X axis. Thus, the initial velocity and its components in the global axis directions are:

$$V_x = \sqrt{2gh} = \sqrt{2 \times 386.4 \frac{\text{in}}{\text{sec}^2} \times 12 \frac{\text{in}}{\text{ft}} \times 30 \text{ft}} = 527.454 \frac{\text{in}}{\text{sec}} \quad (4)$$

The following gravitational load is also applied in the global X direction:

$$G_x = 386.4 \quad (5)$$

The internal pressure applied in the first analysis is inputted again as a constant pressure load in this analysis for the 30-foot drop; namely,

$$P = 500 \text{ psi} \quad (6)$$

Third Analysis for 40-Inch Puncture

The third analysis is to evaluate the structural responses of the cask to a 40-inch drop onto a steel round bar of 6 inches in diameter. The finite-element mesh of the cask and the results of stresses, strains and displacements from the first analysis are imported into this analysis. However, the model of the unyielding floor is not imported, since it is not needed in this 40-inch puncture analysis.

The finite-element model of the round bar is added to this analysis. To simulate a lateral 40-inch puncture, the cask will fall in the positive direction of the global X axis; whereas, the model of the round bar is orientated in the negative direction of the global axis as shown in Figure 6. Figure 7 displays the actual relative positions of the model components after the analytical results of the 30-foot drop is imported from the first analysis as the initial state of the second analysis for the 40-inch puncture.

Boundary Conditions

The boundary conditions given for the second analysis can not be imported and must be refined in the present analysis. The puncture bar is assumed to be fixed at the bottom.

The displacements of the uni-axial connectors should remain constant during the analysis of the 40-inch puncture analysis to simulate the locking of the bolt threads. Thus, the condition given in Equation (3) must also be satisfied in the third analysis.

Initial Velocity and Applied Loads

The third analysis for the 40-inch puncture is not a continuation of the second analysis for the 30-foot drop. The analytical results of the second analysis for the 30-foot drop are imported as the initial state of the present analysis. Thus, the initial velocity for the 40-inch puncture can be directly defined in the present analysis.

Since the falling path of the cask is in the positive direction of the global X axis, the initial velocity of the cask for the 40-inch puncture is:

$$V_0 = \sqrt{2gh} = \sqrt{2 \times 386.4 \frac{\text{in}}{\text{sec}^2} \times 40\text{in}} = 175.818 \frac{\text{in}}{\text{sec}} \quad (6)$$

The following gravitational load is also applied in the positive direction of the global X axis:

$$G_y = 386.4 \frac{\text{in}}{\text{sec}^2} \quad (7)$$

The internal pressure in the third analysis can not be imported from the second analysis. Therefore, it should be redefined in the present analysis as a constant pressure load;

$$P = 500 \text{ psi} \quad (8)$$

DISCUSSION ON ANALYTICAL RESULTS

First Analysis for Bolt Preload and Internal Pressure

Bolt-Tightening Preload, Bolt Axial Forces and Thread Engagement Motions

Figure 8 shows the time-history plots of the bolt-tightening preload forces, bolt axial forces and the displacements due to thread engagements for the full-bolt model, respectively.

The plot shows that the bolt-tightening force (CCF1) of -3000 lbs for the full-bolt model is gradually applied to the connector elements during the period from zero to 0.005 seconds. The plot of the connector displacement (CU1) which represents the thread engagement motion shows a small bump at approximately 0.002 seconds. This bump is caused by the rebound of the closure lid when it first hits the gasket. At the instant of 0.005 seconds, the displacement of the connector element reaches the value of -0.0206 inches and remains at this value afterward. This result indicates that the locking phenomenon of the threads in the bolt and in the bolt hole after the closure tightening is successfully simulated.

During the period from zero to 0.01 seconds, the bolt tensile force (CTF1) increases from zero to the maximum value of 3000 lbs for the full-bolt model. This is the tensile force in the bolts created by bolt-tightening. Furthermore, during the duration from 0.01 seconds to 0.02 seconds, the bolt force increases from 3000 lbs to 4929 lbs for the full-bolt model. The value of 4929 lbs is the bolt tensile force for the combined bolt-tightening preload and the internal pressure.

Stresses Caused by Combined Bolt-Tightening Preload Load and Internal Pressure

Figure 9 shows the contours of von Mises stresses in the overall model. Figure 10 displays the contours of the axial stresses, S22, in the bolts. The results show that the center portions of the bolt stems undergo higher tensile stresses at the inside of the bolt stem surface than at the outside. These stresses can be decomposed into pure bending stresses and uniformly distributed tensile stresses. It is apparent that the uniform tensile stresses are caused by the bolt preload and the internal pressure; whereas the bending stresses are due to the rotation of closure lid and prying effect caused by the internal pressure.

Second Analysis for 30-Foot Drop

Stress Contours:

Figure 11 shows the contours of the von Mises stresses before the 30-foot lateral drop occurs. These stresses are caused by the bolt-tightening preload and the internal pressure and imported from the first analysis.

Figure 12 is the contour plot of the maximum von Mises stress in the cask during the 30-foot drop. Figure 13 is the contour plot of the maximum axial stresses in closure bolt numbers.

Strain Contours

Figures 14 and 15 are the contour plots of the equivalent plastic strains in the containment vessel body and lid, respectively, after a 30-foot drop.

40-Inch Lateral Puncture

Stress Contours:

Figure 16 shows the von Mises Stresses in the cask before the onset of the 40-inch puncture.

The maximum von Mises in the cask during the 40-inch puncture is shown in Figure 17.

Strain Contours:

Figures 18 and 19 depict the contours of the equivalent plastic strains in the containment vessel body and lid, respectively, after the 40-inch puncture.

CONCLUSIONS

A new and improved methodology has been developed for the dynamic analyses of shipping casks subjected to the sequential loading of closure bolt tightening, internal pressure, 30-foot drop and 40-inch puncture.

This methodology has the following advantages over conventional methods:

1. The stresses due to the bolt-tightening preload can be effectively incorporated into the analyses for the subsequent loading
2. The bolt stresses caused by each sequential event, such as bolt-tightening preload, internal pressure and impact loads can be more accurately calculated;
3. The initial velocity of each sequential event in the Hypothetical Accident Conditions (HAC) can be directly defined.
4. The finite-element model of a system component such as an unyielding floor or a punch bar can be added for an impact simulation or removed to avoid obstruction in the impacting path.

REFERENCES

1. Code of Federal Regulations Title 10 part 71 (10CFR71)
2. ABAQUS/Explicit User's Manual, Version 6.8.

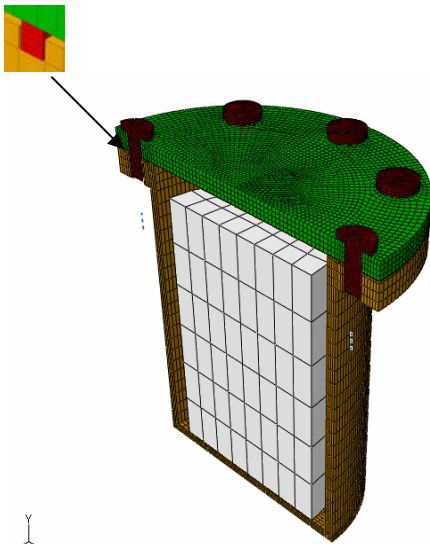


Figure 1. Finite-Element Model for First Analysis

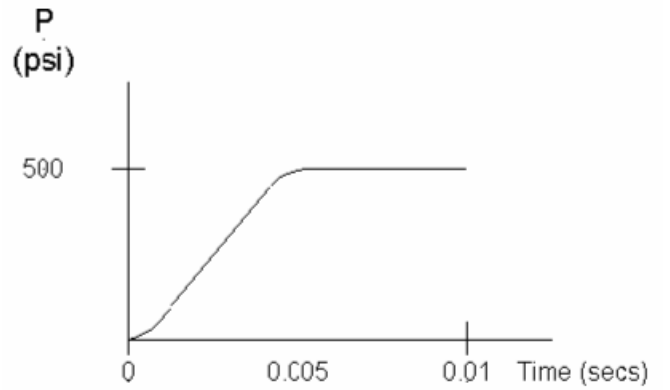


Figure 4. Time History of Internal Pressure

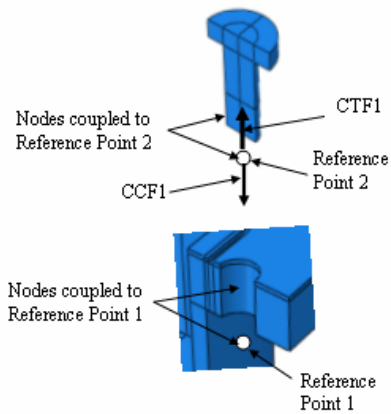


Figure 2. Connector Model for Bolt-Tightening

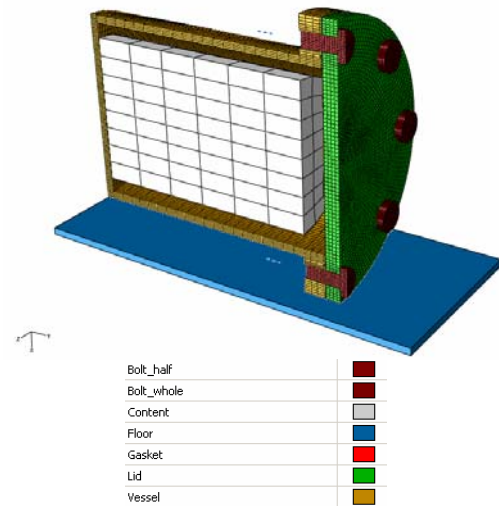


Figure 5. Finite-Element Model for 30-Foot drop

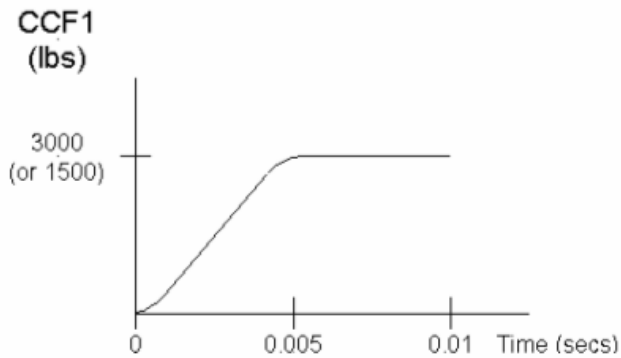


Figure 3. Time History of Bolt-Tightening Load

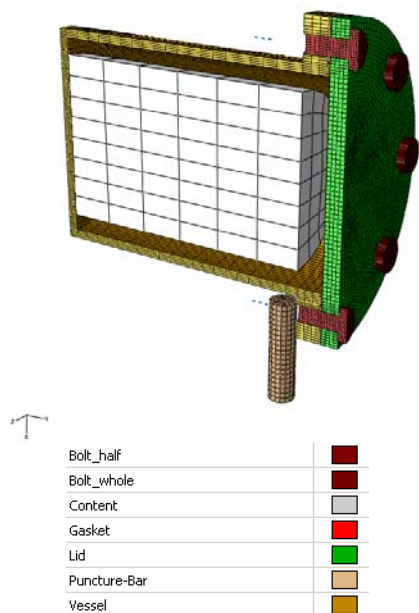


Figure 6. Finite-Element Model for 40-Inch Puncture

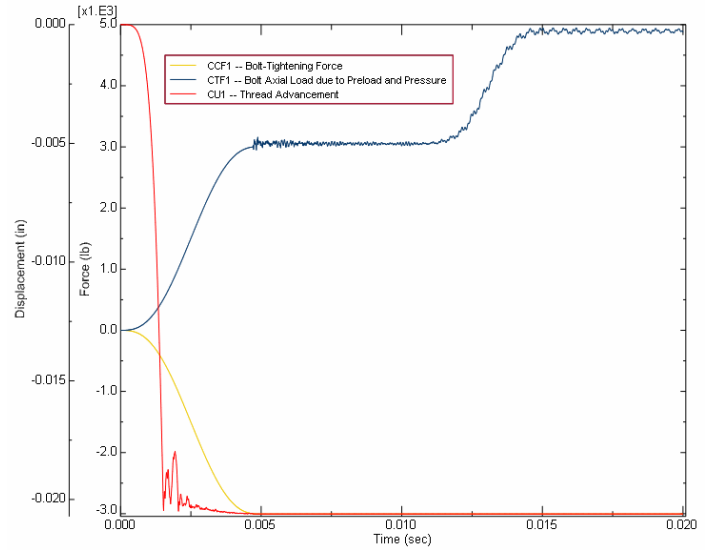


Figure 8. Time Histories of Bolt Axial Forces and Thread Engagement Motion of Full-Bolt Model

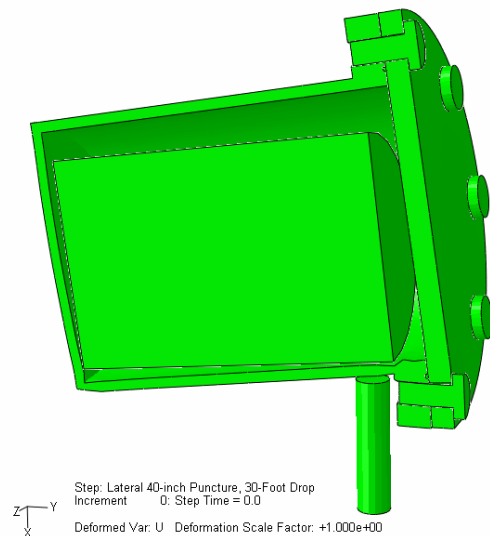


Figure 7. Initial Position of Finite-Element Model for 40-Inch Puncture Analysis

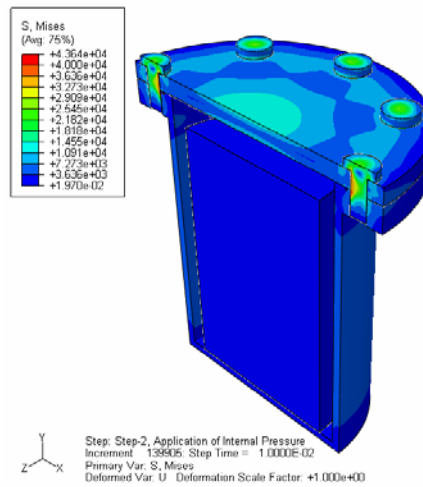


Figure 9. von Mises Stresses in Overall Model Caused by Combined Bolt-Tightening Load and Internal Pressure

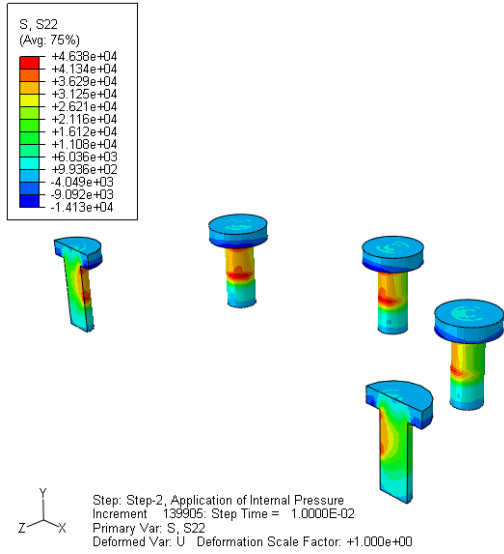


Figure 10. Axial Stresses in Bolts Caused by Combined Bolt-Tightening Load and Internal Pressure

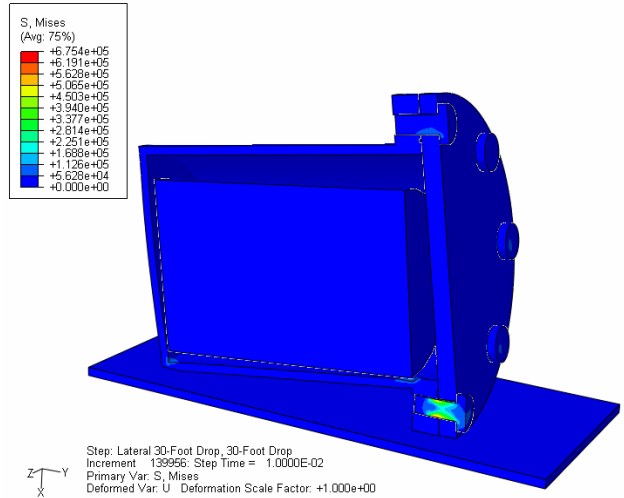


Figure 12. Maximum von Mises Stress in Cask during 30-foot Drop

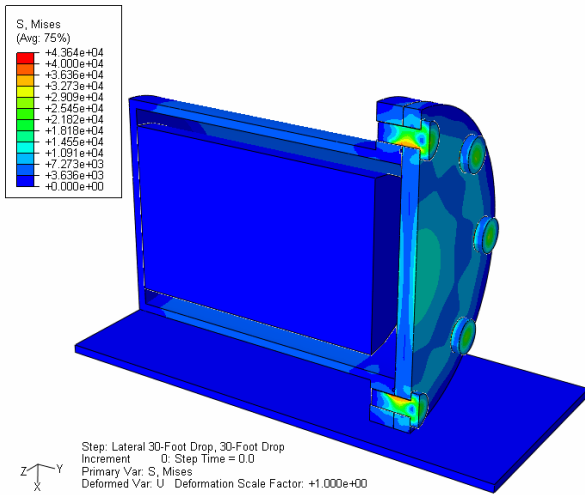


Figure 11. von Mises Stresses before 30-Foot Drop

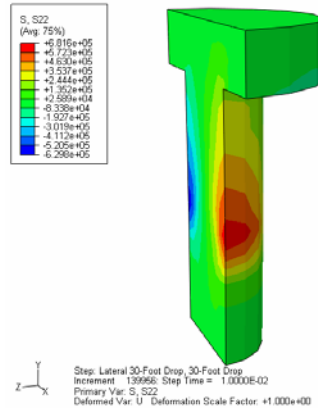


Figure 13. Maximum Axial Tensile Stresses in Closure Bolt

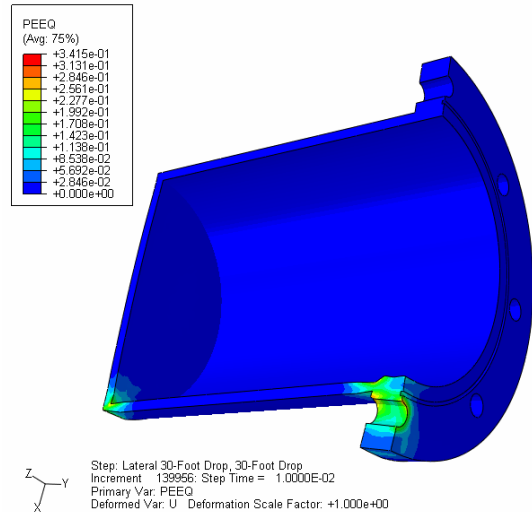


Figure 14. Equivalent Plastic Strains in Containment Vessel Body after 30-foot Drop

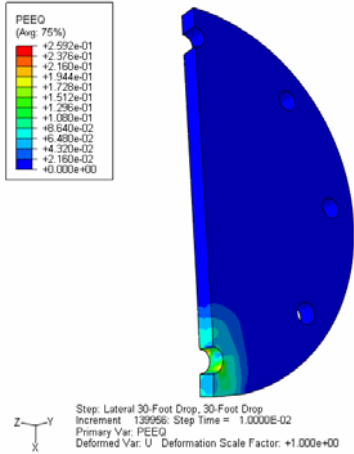


Figure 15. Equivalent Plastic Strains in Containment Vessel Lid after 30-foot drop

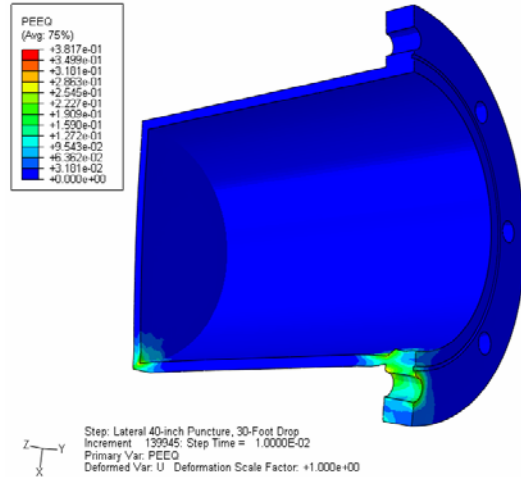


Figure 18. Equivalent Plastic Strain in Containment Vessel Body after 40-inch Puncture

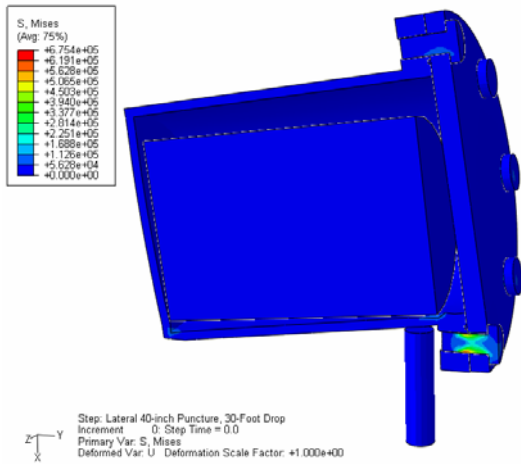


Figure 16. von Mises Stresses in Cask before 40-inch Puncture

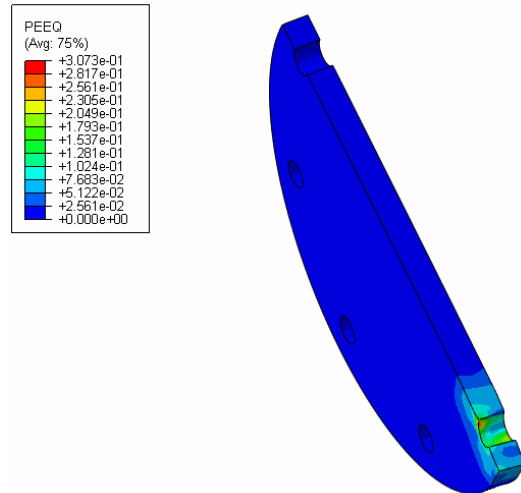


Figure 19. Equivalent Plastic Strains in Containment Vessel Lid after 40-inch Puncture

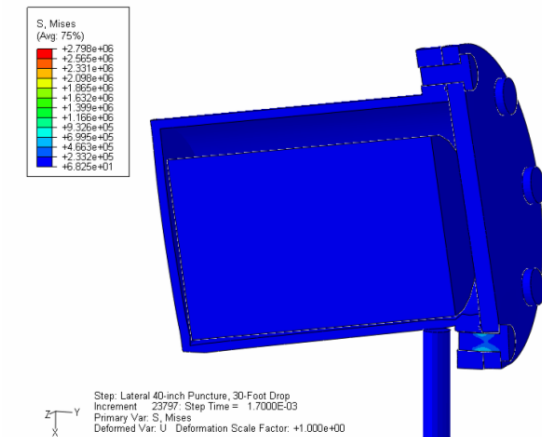


Figure 17. Maximum von Mises Stresses in Cask during 40-inch Puncture